Crystal structures of linear-chain halogen-bridged binuclear platinum complexes, dihydrate forms of $K_4[Pt_2X(pop)_4]\cdot nH_2O$ (X = Cl and Br)

Masahiro Yamashita
College of General Education, Nagoya University, Furocho, Chikusa-ku, Nagoya 464 (Japan)
and **Koshiro Toriumi***
Institute for Molecular Science, Okazaki National Research Institutes, Okazaki 444 (Japan)

(Received April 23, 1990)

Abstract

Crystal structures of the potassium catena-μ-halogenotetrakis(μ-diphosphonato-P,P)-diplatinum(4−) dihydrate, $K_4[Pt_2X(pop)_4]\cdot 2H_2O$ (X = Cl (**1**) and Br (**2**); pop = $P_2O_5H_2^{2-}$), have been determined by the single crystal X-ray diffraction method. The complexes are isomorphous to each other and crystallize in orthorhombic, space group *Pbnm*, $Z = 4$: for **1**, $a = 9.553(2)$, $b = 15.440(3)$, $c = 17.123(3)$ Å, $V = 2525.6(8)$ Å^3 at room temperature; for **2**, $a = 9.510(1)$, $b = 15.338(2)$, $c = 17.125(2)$ Å, $V = 2497.9(6)$ Å^3 at 125 K. The structures consist of linear chains with a repeating unit of $\cdots Pt^{II}$–$Pt^{II}\cdots$X–Pt^{III}–Pt^{III}–X$\cdots$ along the *c* axes. The linear chains are not straight but a little bent to form zigzag chain structures, the bent angles defined by the Pt–Pt bonds and the *c* axes being 3.34(1)° for **1** and 3.11(1)° for **2**, respectively. The Pt–Pt separations, which are bridged by four pyrophosphato ligands ($P_2O_5H_2^{2-}$), are 2.835(1) Å for **1** and 2.834(1) Å for **2**. The bridging halogen atoms are disordered over two sites in the chains, giving short Pt–X and long Pt$\cdots$X separations: 2.406(4) and 3.362(4) Å for **1** and 2.539(1) and 3.217(1) Å for **2**, respectively. The deviations of the bridging halogen atoms from the midpoints between two Pt dimers are significantly larger than those of the trihydrate modifications.

Introduction

Much interest has been focused on the linear-chain halogen-bridged M^{II}–X–M^{IV} mixed valence compounds (M = Pt, Pd or Ni) in the field of solid state physics and chemistry from the viewpoints of low-dimensional materials having extremely strong electron-lattice interactions [1]. They show various characteristic features such as the strong intervalence charge transfer absorption, the resonance Raman spectra with high overtone progression, and the luminescence with large Stokes shifts [2].

The one-dimensional M^{II}–X–M^{IV} compound consists of a linear chain of $\cdots M^{II}\cdots$X–M^{IV}–X$\cdots$, where each halogen atom (X) is not located at the midpoint between two metal atoms but sits on a position closer to the M^{IV} atom [1, 3]. This displacement results in an appearance of a commensurate charge density wave with a period of twice the M$\cdots$M separation. As a result, the half-filled d_{z^2} band directed along the linear chain splits into the fully-occupied valence band and the unoccupied conduction band with a finite energy gap [4]. The relation between the lattice distortion and the band gap has been extensively studied for the mixed valence compounds with both the homo-metal and hetero-metal systems by the various physical measurements such as X-ray crystal structure analyses [3], reflectance, luminescence, resonance Raman spectra [2, 5], electrical conductivity, XANES [6] and XPS [7]. The observed properties have been well interpreted by a theoretical approach proposed by Nasu based on an extended Peierls–Hubbard model [8].

Recently, a new type of halogen-bridged mixed-valence compound, $K_4[Pt_2X(pop)_4]\cdot 3H_2O$ (X = Cl, Br or I), was prepared, which consists of binuclear Pt complexes [9]. The X-ray structure analyses revealed that the crystals consist of a linear chain of a repeating unit of –Pt–Pt–X–Pt–Pt–, where two Pt atoms are bridged by four pyrophosphato ligands and the bridging halogen atoms are deviated from the center between two Pt dimers [10, 11]. Butler *et al.* [11] proposed a mixed valence structure consisting of a $\cdots Pt^{2+}$–$Pt^{2+}\cdots$X–Pt^{3+}–Pt^{3+}–X$\cdots$ re-

*Author to whom correspondence should be addressed.

0020-1693/90/$3.50

peating unit based on the physical properties obtained by the reflectance and resonance Raman spectra, and electrical conductivity measurements, which show semiconductive behavior with smaller activation energies and electrical resistances than those of the halogen-bridged mixed valence compounds consisting of mononuclear Pt complexes [11, 12].

In the course of growing single crystals of the trihydrate compounds, we obtained other crystals with different shapes, which are the dihydrate compounds, $K_4[Pt_2X(pop)_4]\cdot 2H_2O$ (X = Cl or Br). In this paper, the crystal structures of the dihydrate compounds will be described and compared with those of the trihydrate compounds so far reported [10, 11].

Experimental

Syntheses

$K_4[Pt_2X(pop)_4]\cdot 3H_2O$ (X = Cl and Br) were prepared by the method previously reported [9]. Recrystallization of the compounds was made from a small amount of water, to which KCl (**1**) or KBr (**2**) instead of KNO_3 were added. After standing for a week, red or golden column crystals showing strong dichroism were obtained for **1** and **2**, respectively. The dihydrate and trihydrate crystals are easily distinguished under a microscope, since the crystal shape of rhombic columns of the dihydrate crystals appears different from that of tetragonal columns of the trihydrate ones.

X-ray crystal structure analyses

Crystallographic data are summarized in Table 1, along with data collection and refinement information. Intensity data were collected on a Rigaku AFC-5 four circle diffractometer using graphite monochromated Mo Kα radiation, the θ–2θ scan technique being employed. Unit cell dimensions were determined by using 30 2θ values for 1 and 24 for **2** measured on the diffractometer. The intensity data were corrected for Lorentz and polarization factors, and for absorption by a numerical Gaussian integration method.

The structures were solved by a conventional heavy-atom method. The structure of **1** was refined by a block-diagonal least-squares method with anisotropic

TABLE 1. Crystallographic data for $K_4[Pt_2X(P_2O_5H_2)_4]\cdot 2H_2O$

	X = Cl	X = Br
Formula	$Pt_2ClK_4P_8O_{20}H_8\cdot 2H_2O$	$Pt_2BrK_4P_8O_{20}H_8\cdot 2H_2O$
Formula weight	1193.878	1238.33
Crystal system	orthorhombic	orthorhombic
a (Å)	9.553(2)	9.510(1)
b (Å)	15.440(3)	15.338(2)
c (Å)	17.123(3)	17.125(2)
V (Å^3)	2525.6(8)	2497.9(6)
space group	*Pbnm*	*Pbnm*
Z	4	4
D_x (g cm^{-3})	3.140	3.293
μ(Mo Kα) (mm^{-1})	12.983	14.717
Temperature (°C)	25	−152
Crystal		
Color and shape	red rhombic	golden rhombic
Dimensions (mm)	0.12×0.12×0.10	0.16×0.16×0.12
Faces	(110)(1$\bar{1}$0)(001)	(110)(1$\bar{1}$0)(001)
2θ range (°)	$2<2\theta<60$	$2<2\theta<80$
hkl range	$-14<h<14$, $0<k<23$, $0<l<24$	$0<h<17$, $0<k<27$, $0<l<30$
No. reflections measured	8177	8672
No. reflections observed	1937	3620
Transmission factor	0.1869–0.3557	0.0804–0.2287
LS refinement	block-diagonal LS	full-matrix LS
Weighting scheme	$[\sigma^2+(0.007\times\|F\|)^2]^{-1}$	$[\sigma^2+(0.015\times\|F\|)^2]^{-1}$
Extinction correction	none	isotropic
Minimum y		0.84
$R(F)$	0.0283	0.0418
$R_w(F)$	0.0288	0.0417
Goodness of fit	1.464	1.127

thermal parameters for non-hydrogen atoms and **2** by a full-matrix least-squares method. The H atoms could not be located by the difference maps. The scattering factors were taken from the International Tables for X-ray Crystallography [13]. All the calculations were made by the programs of UNICS III [14], RADIEL [15] and ORTEP [16] on a HITAC M680 computer at the Computer Center of the Institute for Molecular Science. Final atomic parameters for **1** and **2** are given in Tables 2 and 3, respectively.

Results and discussion

Description of the linear chain structures

The perspective drawings of the chain structures of **1** and **2** with the atomic numbering systems are presented in Fig. 1(a) and (b), respectively. Relevant interatomic distances and angles are listed in Table 4.

The crystal structures of the chloro-bridged (**1**) and bromo-bridged (**2**) compounds are isomorphous to each other. Two Pt atoms are bridged by four pyrophosphato ligands ($P_2O_5H_2^{2-}$ = pop) to form a binuclear $Pt_2(pop)_4$ unit. The Pt_2 units are also bridged by halogen ions to construct a linear-chain structure along the *c* axes. The linear chains are not straight but a little bent to form zigzag structures,

TABLE 2. Fractional coordinates ($\times 10^5$ for Pt; $\times 10^4$ for others) and equivalent isotropic thermal parameters (Å^2) for **1**

	x	*y*	*z*	B_{eq} [b]
Pt	639(4)	361(2)	8265(2)	1.1
Cl	297(5)	187(3)	2219(2)	2.2
P(1)	−486(3)	1510(1)	791(2)	1.6
P(2)	2457(3)	317(2)	789(1)	1.8
P(3)	612(3)	−1435(1)	899(1)	1.6
P(4)	−2323(3)	−241(1)	946(1)	1.6
O(1)	729(8)	2140(4)	886(4)	2.6
O(2)	−1671(8)	1782(4)	1381(4)	2.3
O(3)	3376(7)	−323(5)	1226(5)	3.5
O(4)	2884(8)	1257(4)	1034(4)	2.6
O(5)	−545(8)	−2070(4)	1105(4)	2.3
O(6)	1924(8)	−1629(4)	1432(4)	2.3
O(7)	−3157(7)	448(5)	1358(4)	3.0
O(8)	−2727(8)	−1154(5)	1273(5)	4.2
O(9)	−1231(7)	1746(3)	−47(4)	1.8
O(10)	3056(7)	262(6)	−88(4)	4.5
K(1)	4978(4)	102(3)	2500	3.4
K(2)	2917(4)	−2833(2)	2500	3.1
K(3)	−505(3)	−3517(1)	113(2)	3.1
W(1)[a]	−182(15)	3258(8)	2500	4.8
W(2)[a]	5067(14)	1911(6)	2500	3.5

[a]Oxygen atoms of water molecules. [b]$B_{eq} = (4/3)\Sigma_i\Sigma_j\beta_{ij}\mathbf{a}_i \cdot \mathbf{a}_j$.

TABLE 3. Fractional coordinates ($\times 10^5$ for Pt; $\times 10^4$ for others) and equivalent isotropic thermal parameters (Å^2) for **2**

	x	*y*	*z*	B_{eq} [b]
Pt	612(3)	327(2)	8262(1)	0.6
Br	261(2)	145(1)	2301(1)	1.0
P(1)	−485(2)	1517(1)	798(1)	0.8
P(2)	2471(2)	315(1)	790(1)	0.9
P(3)	615(2)	−1450(1)	891(1)	0.7
P(4)	−2343(2)	−246(1)	946(1)	0.8
O(1)	722(6)	2145(3)	899(3)	1.0
O(2)	−1663(7)	1795(3)	1393(3)	1.2
O(3)	3392(7)	−327(4)	1221(4)	1.9
O(4)	2891(7)	1262(4)	1046(4)	1.4
O(5)	−535(7)	−2089(3)	1098(4)	1.2
O(6)	1915(6)	−1647(3)	1428(3)	1.1
O(7)	−3198(7)	433(4)	1360(4)	1.5
O(8)	−2751(7)	−1163(4)	1281(5)	2.8
O(9)	−1245(6)	1752(3)	−39(4)	0.9
O(10)	3076(7)	274(6)	−88(4)	3.0
K(1)	4935(3)	133(2)	2500	1.9
K(2)	2939(3)	−2823(2)	2500	1.6
K(3)	−503(2)	−3528(1)	106(1)	1.6
W(1)[a]	−167(12)	3290(6)	2500	2.1
W(2)[a]	5026(12)	1930(5)	2500	1.7

[a]Oxygen atoms of water molecules. [b]$B_{eq} = (4/3)\Sigma_i\Sigma_j\beta_{ij}\mathbf{a}_i \cdot \mathbf{a}_j$.

which are in contrast to the straight chains in the trihydrate compounds of $K_4[Pt_2X(pop)_4]\cdot 3H_2O$ (X = Cl and Br) [10, 11]. The bent angles defined by the Pt–Pt bonds and the *c* axes are 3.34(1)° for **1** and 3.11(1)° for **2**, respectively. As has been observed previously for the trihydrate compounds and for most halogen-bridged M^{II}–X–M^{IV} mixed valence compounds [3], the bridging halogen ions (Cl for **1** and Br for **2**) are disordered over two sites with an occupancy factor of 0.5. The two positions are related by a mirror plane and equidistant from the midpoint between two Pt_2 complexes. The positional disorder gives short Pt–X and long Pt···X distances which can be attributed to the Pt^{III}–X and Pt^{II}···X distances. The observed chain structures can be interpreted by the following two structural models [10], both of which require positional disorder among the chains.

(a) $\cdots Pt^{2+}\text{–}Pt^{2+}\cdots X\text{–}Pt^{3+}\text{–}Pt^{3+}\text{–}X\cdots$

(b) $\cdots Pt^{2+}\text{–}Pt^{3+}\text{–}X\cdots Pt^{2+}\text{–}Pt^{3+}\text{–}X\cdots$

By both the theoretical approach based on a Hückel calculation [17] and physical measurements such as electrical conductivities, magnetic susceptibilities, resonance Raman spectra and electronic spectra [11, 12], it has been revealed that the model of (a) is reasonable for these compounds. Recently, Butler *et al.* redetermined the crystal structures of

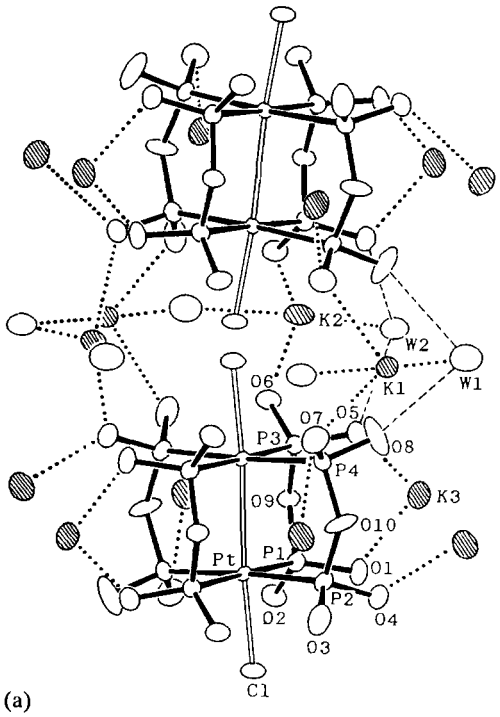

(a)

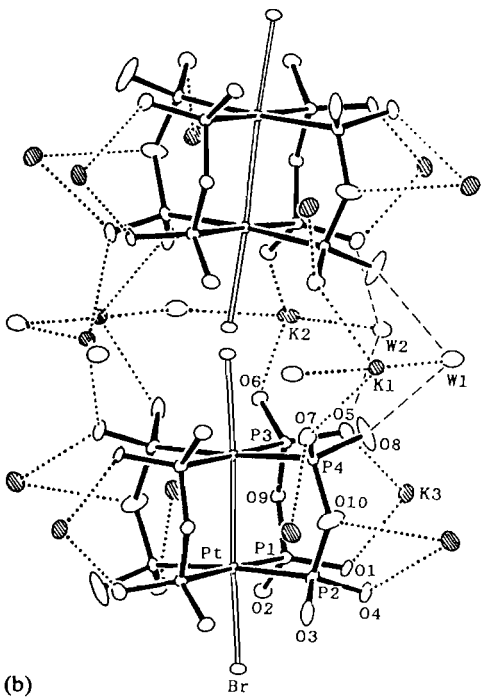

(b)

Fig. 1. ORTEP drawing of a portion of the infinite chain along *c* with surrounding K^+ ions and water molecules of $K_4[Pt_2X(pop)_4]\cdot 2H_2O$ (X = Cl or Br). K^+ ions are drawn by the hatched circles. The dashed lines correspond to hydrogen bonds and the dotted lines to short contacts (less than 3.0 Å) between K^+ ions and O atoms of pop ligands or water molecules. Thermal ellipsoids are 50% probability surfaces. (a) $K_4[Pt_2Cl(pop)_4]\cdot 2H_2O$ (**1**) at room temperature. (b) $K_4[Pt_2Br(pop)_4]\cdot 2H_2O$ (**2**) at 125 K.

TABLE 4. Selected bond distances (Å) and angles (°)

	X = Cl	X = Br
Pt–Pt^i	2.835(1)	2.834(1)
Pt–X	2.406(4)	2.539(1)
Pt···X	3.362(4)	3.217(1)
X···X^i	0.962(6)	0.680(3)
Pt–P(1)	2.337(2)	2.336(2)
Pt–P(2)	2.328(3)	2.333(2)
Pt–P(3)	2.334(2)	2.337(2)
Pt–P(4)	2.329(3)	2.334(2)
P(1)–O(1)	1.523(7)	1.509(6)
P(2)–O(3)	1.519(8)	1.511(7)
P(3)–O(5)	1.519(7)	1.511(6)
P(4)–O(7)	1.505(8)	1.500(6)
P(1)–O(2)	1.571(8)	1.574(6)
P(2)–O(4)	1.565(7)	1.569(6)
P(3)–O(6)	1.579(8)	1.571(6)
P(4)–O(8)	1.565(8)	1.568(7)
P(1)–O(9)	1.642(8)	1.644(6)
P(2)–O(10)	1.609(8)	1.611(7)
P(3)–O(9)^i	1.646(8)	1.643(6)
P(4)–O(10)^i	1.629(8)	1.627(7)
X–Pt–Pt^i	175.6(1)	177.31(3)
X–Pt–P(1)	87.3(1)	88.37(6)
X–Pt–P(2)	85.3(1)	86.58(6)
X–Pt–P(3)	91.2(1)	90.12(6)
X–Pt–P(4)	91.2(1)	89.92(6)
P(1)–Pt–P(2)	92.21(9)	92.14(7)
P(1)–Pt–P(4)	87.79(9)	87.84(7)
P(2)–Pt–P(3)	87.85(9)	87.84(7)
P(3)–Pt–P(4)	92.06(9)	92.20(7)
P(1)–Pt–P(3)	178.42(9)	178.49(7)
P(2)–Pt–P(4)	176.53(9)	176.50(8)
Pt–P(1)–O(1)	116.6(3)	116.8(2)
Pt–P(2)–O(3)	115.7(3)	115.8(3)
Pt–P(3)–O(5)	118.5(3)	118.7(3)
Pt–P(4)–O(7)	115.4(3)	116.5(3)
Pt–P(1)–O(2)	113.9(3)	114.1(2)
Pt–P(2)–O(4)	114.9(3)	114.5(2)
Pt–P(3)–O(6)	113.2(3)	113.1(2)
Pt–P(4)–O(8)	116.0(3)	116.0(3)
Pt–P(1)–O(9)	109.6(2)	109.3(2)
Pt–P(2)–O(10)	111.4(3)	111.6(3)
Pt–P(3)–O(9)^i	108.5(2)	108.3(2)
Pt–P(4)–O(10)^i	110.2(3)	110.2(3)
O(1)–P(1)–O(2)	108.0(4)	107.1(3)
O(3)–P(2)–O(4)	108.7(4)	108.6(4)
O(5)–P(3)–O(6)	108.7(4)	107.9(3)
O(7)–P(4)–O(8)	109.8(4)	108.4(4)
O(1)–P(1)–O(9)	106.4(4)	107.1(3)
O(3)–P(2)–O(10)	102.7(4)	102.9(4)
O(5)–P(3)–O(9)^i	106.2(4)	106.9(3)
O(7)–P(4)–O(10)^i	102.1(4)	102.3(3)
O(2)–P(1)–O(9)	101.0(4)	101.1(3)
O(4)–P(2)–O(10)	101.9(4)	101.8(3)
O(6)–P(3)–O(9)^i	99.9(4)	100.3(3)
O(8)–P(4)–O(10)^i	101.6(5)	101.5(4)
P(1)–O(9)–P(3)^i	123.7(4)	123.5(3)
P(2)–O(10)–P(4)^i	133.7(5)	133.7(5)

Key to symmetry operations: (i) $-x$, $-y$, $-z$.

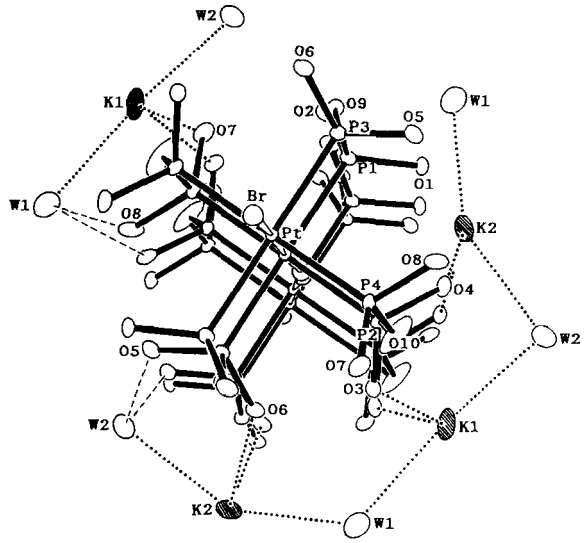

Fig. 2. Arrangement of K^+ ions and water molecules around the infinite chain of $K_4[Pt_2Br(pop)_4]\cdot 2H_2O$ (**2**). Positions of K(3) are omitted for clarity. Details are the same as Fig. 1.

$K_4[Pt_2X(pop)_4]\cdot 3H_2O$ (X = Cl and Br) at 22 and 19 K, respectively, and demonstrated the chain structure of (a) [11].

The Pt–Pt separations of the Pt_2 dimer units are 2.835(1) Å for **1** and 2.834(1) Å for **2**, which are intermediate between those of the corresponding Pt^{II}–Pt^{II} [18] and Pt^{III}–Pt^{III} complexes [9, 10] having discrete structures. The Pt–Pt distances decrease as the formal oxidation states of the platinum atoms increase, which is consistent with the number of 5d electrons occupying Pt–Pt antibonding orbitals: $(d\sigma)^2(d\sigma^*)^2$ for the discrete Pt^{II}–Pt^{II} complex of $K_4[Pt_2(pop)_4]\cdot 2H_2O$, $(d\sigma)^2(d\sigma^*)^1$ for the linear chain Pt^{II}–Pt^{II}–X–Pt^{III}–Pt^{III} compounds of $K_4[Pt_2X(pop)_4]\cdot 2H_2O$, and $(d\sigma)^2(d\sigma^*)^0$ for the discrete X–Pt^{III}–Pt^{III}–X complexes of $K_4[Pt_2X_2(pop)_4]\cdot 2H_2O$ [19]. Although the observed Pt–Pt distances should be the average distance given by a superposition of Pt^{II}–Pt^{II} and Pt^{III}–Pt^{III} distances, any anomaly could not be observed in the thermal ellipsoid of the Pt atom.

The Pt–X distances (2.406(4) Å for **1** and 2.539(1) Å for **2**) are almost equal to those of the discrete complexes of $K_4[Pt_2X_2(pop)_4]\cdot 2H_2O$ (2.407(2) Å for X = Cl and 2.555(5) Å for X = Br) [9, 10]. Because of the disordered structure described previously, the observed Pt–X distances may correspond to the distance between the bridging halogen ion and the average position of Pt^{II} and Pt^{III} atoms, giving a shorter distance than the true values in the crystals. Accordingly, it may be reasonable to assume that the Pt^{III}–X distance in the chain structure is slightly longer than that of the discrete Pt^{III} binuclear complexes. A similar trend has been reported for the M^{II}–X–M^{IV} compounds [20].

As shown in Fig. 2, the bridging O atom of the $P_2O_5H_2^{2-}$ ligand deviates from the ligand plane defined by the two Pt atoms and the two P atoms of the ligand. This ligand structure is similar to that of the ammonium salts of $(NH_4)_4[Pt_2X(pop)_4]$ (X = Cl or Br) [21] but is significantly different from the planar structure of the trihydrate modifications [10, 11]. In the trihydrate compounds, thermal ellipsoids of the bridging O atoms are largely elongated per-

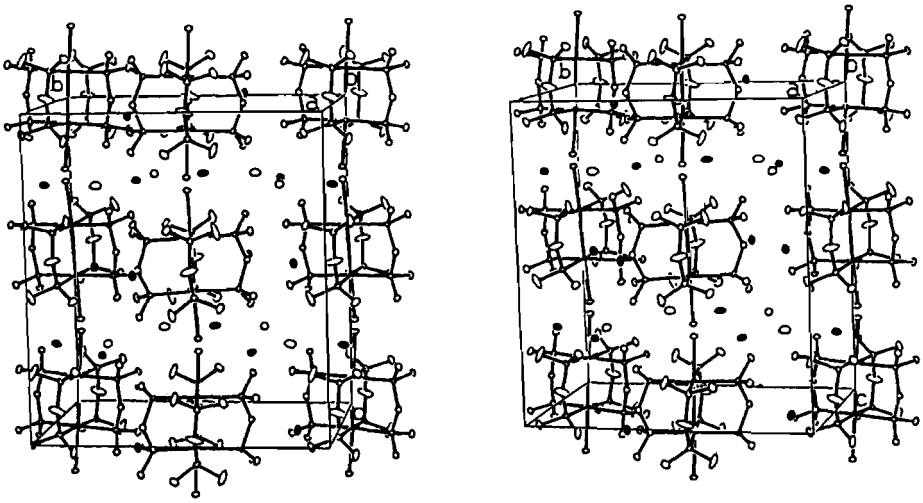

Fig. 3. Stereoscopic view of the crystal structure of $K_4[Pt_2Br(pop)_4]\cdot 2H_2O$ (**2**) at 125 K. The hatched circles correspond to K^+ ions. Thermal ellipsoids are 50% probability surfaces.

pendicular to the ligand planes, indicating a large positional disorder of the structures.

Description of the crystal packings

A stereoscopic view of the crystal structure of **2** is shown in Fig. 3, since the crystals of **1** and **2** are isomorphous to each other. Potassium cations and waters of crystallization play important roles in the formation of the halogen-bridged linear-chain structure. As shown in Figs. 1 and 2, the potassium ions and waters are arranged around the linear chain. The short contacts between K^+ ions and oxygen atoms of the pop ligands are listed in Table 5, along with the hydrogen bond distances. The Pt_2 units bridged by a halogen ion are bound to each other by electrostatic interaction through the potassium cations which attract oxygen atoms of the pop ligands.

TABLE 5. Short contacts (Å) among the Pt dimer anions, K^+ cations and water molecules. The distances less than 3.0 Å for K···O and 3.1 Å for O···O are listed

	X = Cl	X = Br
K(1)···W(1)^{i}	2.853(12)	2.835(10)
K(1)···W(2)^{iv}	2.795(11)	2.756(8)
K(1)···O(3)^{iv}	2.743(8)	2.730(7)
K(1)···O(7)^{v}	2.700(8)	2.679(7)
K(2)···W(1)^{i}	2.742(14)	2.722(11)
K(2)···W(2)^{i}	2.878(14)	2.845(11)
K(2)···O(4)^{i}	2.976(7)	2.965(6)
K(2)···O(6)^{iv}	2.775(7)	2.751(6)
K(3)···O(1)^{vi}	2.738(7)	2.740(6)
K(3)···O(4)^{vii}	2.979(8)	2.977(7)
K(3)···O(5)	2.808(7)	2.785(6)
K(3)···O(7)^{viii}	2.954(8)	2.945(6)
K(3)···O(10)^{vii}		2.968(8)
W(1)···O(8)^{ii}	3.038(13)	2.997(11)
W(2)···O(5)^{iii}	2.896(9)	2.874(7)

Key to symmetry operations: (i) $\frac{1}{2}-x, -\frac{1}{2}+y, \frac{1}{2}-z$; (ii) $-\frac{1}{2}-x, \frac{1}{2}+y, \frac{1}{2}-z$; (iii) $\frac{1}{2}-x, \frac{1}{2}+y, \frac{1}{2}-z$; (iv) x, y, $\frac{1}{2}-z$; (v) $1+x, y, \frac{1}{2}-z$; (vi) $-x, -y, -z$; (vii) $\frac{1}{2}-x, -\frac{1}{2}+y, z$; (viii) $-\frac{1}{2}-x, -\frac{1}{2}+y, z$.

Waters of crystallization sit on a mirror plane which is perpendicular to the linear chain and located at the midpoint between two Pt_2 units. They interact via electrostatic forces with the potassium ions in the same plane, constructing a two-dimensional network. The arrangements of the potassium ions and waters in the dihydrate crystals are not symmetric around the linear chains, which are in contrast to the symmetric structures in the trihydrate crystals [10, 11]. This is responsible for the bending structures of linear chains in the dihydrate compounds. Each linear chain is also linked by the potassium ions.

Lattice distortions in the one-dimensional compounds

In the halogen-bridged mixed valence compounds having a one-dimensional linear-chain structure, the bridging halogen ion is located at a position just deviated from the midpoint between two metal atoms toward the metal atom having the higher oxidation state. This deviation is considered to be a lattice distortion due to the Peierls instability of one-dimensional compounds. Structural parameters along the linear chains of the $[Pt_2X(pop)_4]^{4-}$ compounds are summarized in Table 6. In order to compare the lattice distortion, it may be useful to define a parameter R which is given by the ratio between the shorter Pt–X and the longer Pt···X distances. The lattice distortions of R for the bromo-bridged compounds are significantly larger than those for the corresponding chloro-bridged compounds. On the other hand, comparing the R values among the compounds having the same bridging halogen ion, the dihydrate compounds show smaller R values than the trihydrate compounds and further the ammonium salts. It may be also noted that the Pt–Pt distances decrease as the R values increase. When the crystal packings of the dihydrate and trihydrate compounds are compared, they reveal that interactions between the K^+ ions and waters of crystallization in the

TABLE 6. Comparison of the interatomic distances along chains (Å)

Compound	Pt–Pt	Pt–X	Pt···X	Pt–P	R^a	Reference
$K_4[Pt^{II}_2(pop)_4]\cdot 2H_2O$	2.925(1)			2.320(5)		18
$K_4[Pt^{III}_2Cl_2(pop)_4]\cdot 2H_2O$	2.695(1)	2.407(2)		2.350(2)		9
$K_4[Pt^{III}_2Br_2(pop)_4]\cdot 2H_2O$	2.723(4)	2.555(5)		2.342(4)		10
$K_4[Pt_2Cl(pop)_4]\cdot 3H_2O$	2.813(1)	2.367(7)	2.966(8)	2.329(3)	0.80	10
$K_4[Pt_2Cl(pop)_4]\cdot 2H_2O$	2.835(1)	2.406(4)	3.362(4)	2.332(4)	0.72	this work
$(NH_4)_4[Pt_2Cl(pop)_4]$	2.830(1)	2.363(4)	3.022(4)	2.328(9)	0.78	21
$K_4[Pt_2Br(pop)_4]\cdot 3H_2O$	2.781(1)	2.579(4)	2.778(4)	2.331(1)	0.93	9, 11
$K_4[Pt_2Br(pop)_4]\cdot 2H_2O$	2.834(1)	2.539(1)	3.217(1)	2.335(2)	0.79	this work
$(NH_4)_4[Pt_2Br(pop)_4]$	2.823(1)	2.513(3)	3.006(3)	2.332(7)	0.84	21

[a] R is defined by the ratio of distances (Pt–X)/(Pt···X).

dihydrates are apparently stronger than those in the trihydrates. This is easily understood by the fact that the thermal ellipsoids of waters in the trihydrates are exceptionally large [9–11]. The strong interaction between K^+ and waters should give rise to weak interaction between the Pt_2 dimers through the K^+, which corresponds to the large lattice distortion in the dihydrate compounds.

These facts strongly suggest that both the kind and arrangement of the counter-ions and also of solvents of crystallization play an important role in the Peierls distortion of the linear chain structures, and also in their solid state properties.

Physical measurements for the dihydrate compounds are now in progress.

Supplementary material

Tables S-I to S-IV giving anisotropic thermal factors and a listing of observed and calculated structure factors are available from the authors on request.

References

1 J. S. Miller and A. J. Epstein, in S. J. Lippard (ed.), *Progress in Inorganic Chemistry,* Vol. 20, Wiley, New York, 1976, p. 1; H. J. Keller, in J. S. Miller (ed.), *Extended Linear Chain Compounds,* Vol. 1, Plenum, New York, 1982, p. 357.

2 R. J. H. Clark, *Advances in Infrared and Raman Spectroscopy,* Vol. 11, Heyden, London, 1984, p. 95; H. Tanino and K. Kobayashi, *J. Phys. Soc. Jpn., 52* (1983) 1446; Y. Wada, T. Mitani, M. Yamashita and T. Koda, *J. Phys. Soc. Jpn., 54* 1985) 3143.

3 B. M. Craven and D. Hall, *Acta Crystallogr., 14* (1961) 475; M. Yamashita, K. Toriumi and T. Ito, *Acta Crystallogr., Sect. C, 42* (1985) 876; K. Toriumi, M. Yamashita and I. Murase, *Chem. Lett.,* (1986) 1753; A. L. Beauchamp, D. Layek and T. Theophanides, *Acta Crystallogr., Sect. B, 38* (1982) 1158.

4 M.-H. Whangbo and M. J. Foshee, *Inorg. Chem., 20* (1981) 113.

5 M. Yamashita, I. Murase, T. Ito, Y. Wada, T. Mitani and I. Ikemoto, *Bull. Chem. Soc. Jpn., 58* (1985) 2336; Y. Wada, K. Toriumi, T. Mitani and M. Yamashita, *J. Phys. Soc. Jpn., 58* (1989) 3013.

6 H. Tanino, H. Oyanagi, M. Yamashita and K. Kobayashi, *Solid State Commun., 53* (1985) 953; H. Tanino, N. Koshizuka, K. Hoh, K. Kato, M. Yamashita and K. Kobayashi, *Physica, 139 & 140B* (1986) 487.

7 M. Yamashita, N. Matsumoto and S. Kida, *Inorg. Chim. Acta, 31* (1978) L381; M. Yamashita and T. Ito, *Inorg. Chim. Acta, 87* (1984) L5.

8 K. Nasu, *J. Phys. Soc. Jpn., 52* (1983) 3865; *53* (1984) 302; *53* (1984) 427.

9 C.-M. Che, F. H. Herbstein, W. P. Schaefer, R. E. Marsh and H. B. Gray, *J. Am. Chem. Soc., 105* (1983) 4604.

10 R. J. H. Clark, M. Kurmoo, H. M. Dawes and M. B. Hursthouse, *Inorg. Chem., 25* (1986) 409.

11 L. G. Butler, M. H. Zietlow, C.-M. Che, W. P. Schaefer, S. Sridhar, P. J. Grunthaner, B. I. Swanson, R. J. H. Clark and H. B. Gray, *J. Am. Chem. Soc., 110* (1988) 1155.

12 M. Kurmoo and R. J. H. Clark, *Inorg. Chem., 24* (1985) 4420; M. A. Strond, H. G. Drickamer, M. H. Zietlow, H. B. Gray and B. I. Swanson, *J. Am. Chem. Soc., 111* (1989) 66.

13 *International Tables for X-ray Crystallography,* Vol. IV, Kynoch Press, Birmingham, 1974, pp. 71–98, 149.

14 T. Sakurai and K. Kobayashi, *Rikagaku Kenkyuusho Hokoku (Rep. Inst. Phys. Chem. Res.), 55* (1979) 69.

15 P. Coppens, T. N. Guru Row, P. Leung, E. D. Stevens, P. J. Becker and Y. W. Yang, *Acta Crystallogr., Sect. A, 35* (1979) 63.

16 C. K. Johnson, *ORTEP, Rep. ORNL-3794,* Oak Ridge National Laboratory, TN, U.S.A., 1965.

17 M.-H. Whangbo and E. Canadell, *Inorg. Chem., 25* (1986) 1726.

18 M. A. Filomena Dos Remedios Pinto, P. J. Sadler, S. Neidle, M. R. Sanderson, A. Subbiah and R. Kuroda, *J. Chem. Soc., Chem. Commun.,* (1980) 13; R. E. Marsh and F. H. Herbstein, *Acta Crystallogr., Sect. B, 39* (1983) 280.

19 C.-M. Che, W. P. Schaefer, H. B. Gray, M. K. Dickson, P. B. Stein and D. M. Roundhill, *J. Am. Chem. Soc., 104* (1982) 4253.

20 K. Toriumi, M. Yamashita, H. Ito and T. Ito, *Acta Crystallogr., Sect. C, 42* (1986) 963.

21 S. Jin, T. Ito, K. Toriumi and M. Yamashita, *Acta Crystallogr., Sect. C, 45* (1989) 1415; K. Toriumi, M. Yamashita, S. Jin and T. Ito, *Acta Crystallogr.,* to be published.